PROCEEDINGS OF SCIENCE

Top physics

S.Bifani

University of Birmingham, School of Physics and Astronomy, Birmingham, United Kingdom

M.Franchini

Istituto Nazionale Di Fisica Nucleare, Sezione di Bologna, Bologna, Italy

A.O.M.Iorio

Istituto Nazionale Di Fisica Nucleare, Sezione di Napoli, Napoli, Italy

An overview of top quark measurements at LHC is presented, including results from Run-I and Run-II. Inclusive and differential cross-section measurements of top quarks produced singly and in pairs are shown from the ATLAS, CMS, and LHCb collaborations. Measurements of top quark properties, both in production and decay, are presented, as well as their interpretation in terms of searches for new physics beyond the Standard Model. Finally, top quark mass measurements are illustrated.

VII Workshop italiano sulla fisica pp a LHC
16-18 Maggio 2016
Pisa, Italy

PoS(PP@LHC2016)019

1. Inclusive production

In proton-proton collisions top quarks are primarily produced via the strong interaction as $q\bar{q}$ pairs, and gluon-gluon fusion accounts for approximately 80% of the total. The measurement of the inclusive $t\bar{t}$ cross-section, $\sigma_{t\bar{t}}$, provides an important test of perturbative Quantum Chromodynamics (QCD) and is sensitive to the strong coupling constant, the gluon parton distribution function (PDF), the top quark mass and new physics models. Furthermore, top production is also one of the main source of backgrounds in many searches for physics beyond the Standard Model(SM), and therefore the study of its production and decay properties forms a core part of the LHC physics program.

Inclusive cross-section measurements are of particular importance as theoretical calculations are nowadays available with a precision of 5–10% [1], a level which is comparable to recent experimental measurements. A variety of decay topologies is used by the ATLAS and CMS collaborations to determine the inclusive $t\bar{t}$ production cross-section, where the most precise results are obtained by using events with an opposite-charge isolated electron and muon pair and additional b-tagged jets. The LHCb experiments can provide additional insight to the production in the forward direction, but only the final state with a single muon and a b-tagged jet is statistically accessible in the Run-I data set because of the lower rate of luminosity and smaller fiducial acceptance than the general purpose detectors.

The cross-section for $t\bar{t}$ production at $\sqrt{s} = 7$, 8 [5] and 13 TeV [6] is measured by the ATLAS collaboration using datasets corresponding to an integrated luminosities of 4.6, 20.3 and 3.2 fb^{-1}. A pure sample of $t\bar{t}$ events is preselected by requiring one electron and one opposite-charge muon with a $p_T > 25$ GeV and $|\eta| < 2.5$. Jets are subsequently identified as likely to originate from the fragmentation of a b-quark using a multivariate technique. The numbers of events with one and two b-tagged jets are counted and used to simultaneously determine the $t\bar{t}$ cross-section and the efficiency to reconstruct and identify a b-jet, which minimise the associated systematic uncertainties. The distribution of the number of identified b-jets is shown for the $\sqrt{s} = 13$ TeV event sample in Figure 1(a). The cross-section for $t\bar{t}$ production is measured to be

$$\begin{aligned}
\sigma_{t\bar{t}}^{7\text{TeV}} &= 182.9 \pm 3.1(\text{stat}) \pm 4.2(\text{syst}) \pm 3.6(\text{lumi}) \pm 3.3(\text{beam})\text{pb}, \\
\sigma_{t\bar{t}}^{8\text{TeV}} &= 242.4 \pm 1.7(\text{stat}) \pm 5.5(\text{syst}) \pm 7.5(\text{lumi}) \pm 4.2(\text{beam})\text{pb}, \\
\sigma_{t\bar{t}}^{13\text{TeV}} &= 818 \pm 8(\text{stat}) \pm 27(\text{syst}) \pm 19(\text{lumi}) \pm 12(\text{beam})\text{pb}.
\end{aligned}$$

The $t\bar{t}$ cross-section evolution with the centre-of-mass energy is presented in Fig. 1(b). A further reduction of systematic uncertainties is achieved by measuring the ratio of the $t\bar{t}$ and Z boson production cross-sections [7].

$$R_{t\bar{t}}^{13\text{TeV}}/Z = 0.445 \pm 0.027(\text{stat}) \pm 0.028(\text{syst}).$$

where the uncertainty on the integrated luminosity almost completely cancels. The results are consistent with recent theoretical QCD calculations at NNLO.

The CMS collaboration measured the $t\bar{t}$ cross-section in the $\sqrt{s} = 7$, 8 [8] and 13 TeV [9] datasets using integrated luminosities of 5.0, 19.7 and 2.2 fb^{-1}. Events containing an $e\mu$ pair are selected without any jet requirements. An extended binned likelihood fit is performed on several

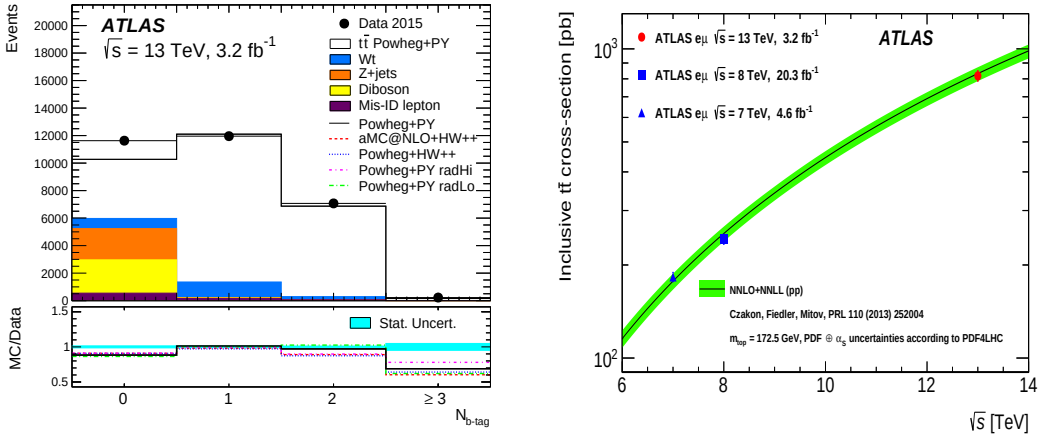

(a) (b)

Figure 1: Distribution of the number of b-tagged jets in preselected opposite-sign $e\mu$ events compared to simulation (a). Cross-section for $t\bar{t}$ pair production in pp collisions as a function of centre-of-mass energy compared to the NNLO+NNLL theoretical predictions (b) [6].

sub-categories of events classified according to the number of jets and b-jets they contain. The distribution of the number of identified b-jets is shown for the $\sqrt{s} = 13$ TeV event sample in Figure 2(a). The cross-section for $t\bar{t}$ production is measured to be

$$\sigma_{t\bar{t}}^{7\text{TeV}} = 173.6 \pm 2.1(\text{stat})^{+4.5}_{-4.0}(\text{syst}) \pm 3.8(\text{lumi})\text{pb},$$
$$\sigma_{t\bar{t}}^{8\text{TeV}} = 244.9 \pm 1.4(\text{stat})^{+6.3}_{-5.5}(\text{syst}) \pm 6.4(\text{lumi})\text{pb},$$
$$\sigma_{t\bar{t}}^{13\text{TeV}} = 793 \pm 8(\text{stat}) \pm 38(\text{syst}) \pm 21(\text{lumi})\text{pb}.$$

For the latter result, a cut-and-count approach is followed rather than a maximum likelihood fit in order to extract the signal cross section. The $t\bar{t}$ cross-section evolution with the centre-of-mass energy is presented in Figure 2(b). The results are consistent with recent theoretical QCD calculations at NNLO.

The cross-section for top production at $\sqrt{s} = 7$ and 8 TeV [10] is measured by the LHCb collaboration using datasets corresponding to an integrated luminosities of approximately 1 and 2fb^{-1}. Events are required to contain one forward muon, $2 < \eta < 4.5$, and one forward b-jet, $2.2 < \eta < 4.2$, with transverse momentum greater than 25 GeV and in the range 50-100 GeV, respectively. The b-tagging is performed using the secondary vertex tagger algorithm described in [11], and the sample purity is determined using a template fit to the muon isolation.

The significance of the top quark contribution to the selected data sample is determined by comparing the observed event yield and charge asymmetry to the SM prediction with and without the contribution from top quark production. The distribution of the transverse momentum of the μ and b-jet pair is shown in Figure 3(a). A significance of 5.4σ is obtained, confirming the observation of top quark production in the forward region. The excess is used to calculate the cross-section for top quark production, which includes contributions from both $t\bar{t}$ and single-top-quark

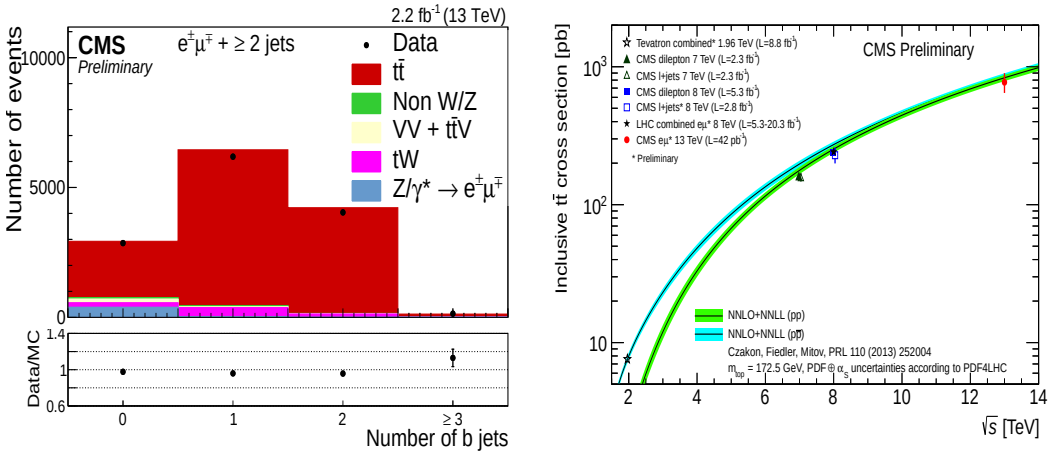

(a) (b)

Figure 2: Distribution of the number of b-tagged jets in preselected opposite-sign $e\mu$ events compared to simulation (a). Cross-section for $t\bar{t}$ pair production in pp collisions as a function of centre-of-mass energy compared to the NNLO+NNLL theoretical predictions (b)CMS [9].

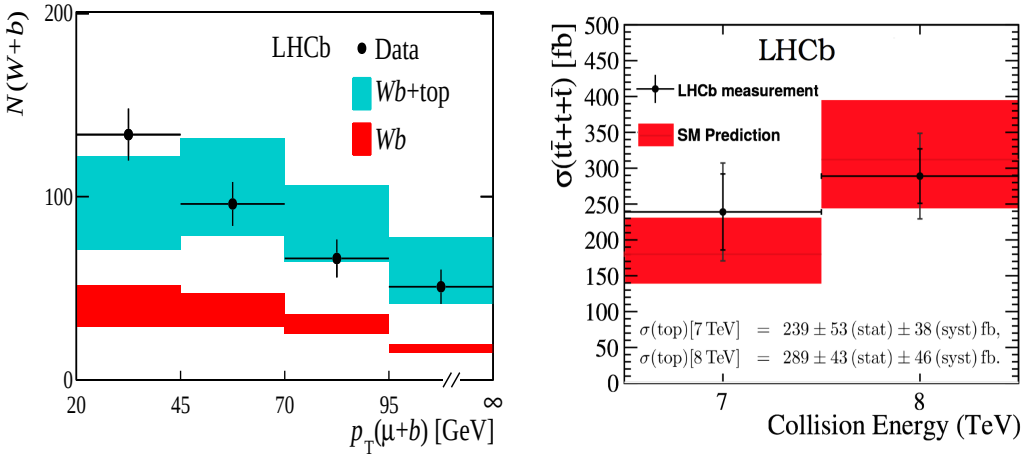

(a) (b)

Figure 3: Distribution of the transverse momentum of the μ and b-jet pair compared to SM predictions at NLO calculated with and without the contribution from top quark production (a). Cross-section for $t\bar{t}$ pair production in pp collisions as a function of centre-of-mass energy (b) [10].

production

$$\sigma_{t\bar{t}}^{7\text{TeV}} = 239 \pm 53(\text{stat})33(\text{syst}) \pm 24(\text{theory})\text{fb},$$
$$\sigma_{t\bar{t}}^{8\text{TeV}} = 289 \pm 43(\text{stat})40(\text{syst}) \pm 29(\text{theory})\text{fb}.$$

The $t\bar{t}$ cross-section evolution with the centre-of-mass energy is presented in Figure 3(b). The results are consistent with recent theoretical QCD calculations at NLO.

2. Associated production $t\bar{t}$+jets

Final states of proton-proton collisions at LHC often include jets arising from QCD bremsstrahlung

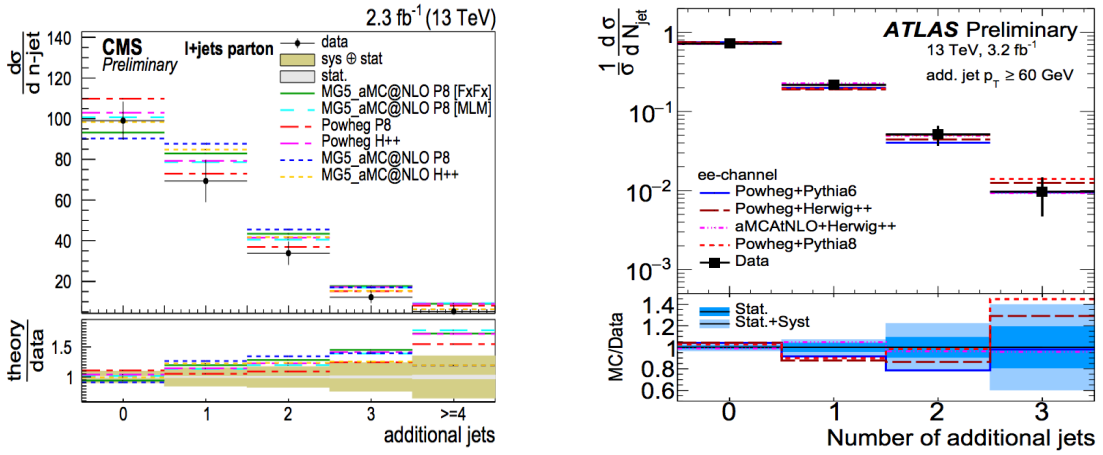

(a) (b)

Figure 4: $t\bar{t}$ production cross section as a function of the number of additional jets from CMS (a) [13] and ATLAS (b) [12].

due to the strongly interacting partons in the initial state and the high centre-of-mass energy of the scattering process. The measurement of jet multiplicity in top quark-antiquark pair final states is sensitive to the production mechanism of additional jets coming from QCD bremsstrahlung.

The normalised differential cross-sections of top-quark pair production as a function of the multiplicity of additional jets is measured by both ATLAS [12] and CMS [13][14] using the latest pp collision data at a centre-of-mass energy of 13 TeV with a luminosity of 3.2 fb^{-1} and 2.3 fb^{-1} respectively. The measurements from both experiments are presented at particle-level fiducial phase space in order to reduce the model dependent uncertainties. CMS also extended the results at the parton level. The measurements presented by ATLAS is performed in the di-lepton channel, where both the top quarks decay to leptonic final states. CMS, instead, measured the cross section in the lepton-plus-jets channel where one top quark decays leptonically and the other hadronically. The $t\bar{t}$ production cross-section measured by CMS appears to be compatible with all the Standard Model predictions considered. The uncertainty on the result at parton level is dominated by the theoretical modeling while at particle level jet energy calibration and b-tagging efficiency are the main source of uncertainty.

Consistency within the statistical uncertainty is found between the data and theoretical predictions and between different di-lepton channels also in the ATLAS result. However, is has to be noted the Powheg+Pythia6 predictions are systematically below the data at high multiplicity. This difference is probably due to the tuning of the Parton Shower simulation at which this measure is particularly sensitive.

Even if both the ATLAS and CMS results in Figures 4 are in agreement with the predictions within the uncertainty, it has to be noted that an opposite trend in the differential result is present. In the ATLAS result, the MC events underestimates the data in the high jet-multiplicity region, while CMS results behave in the opposite way.

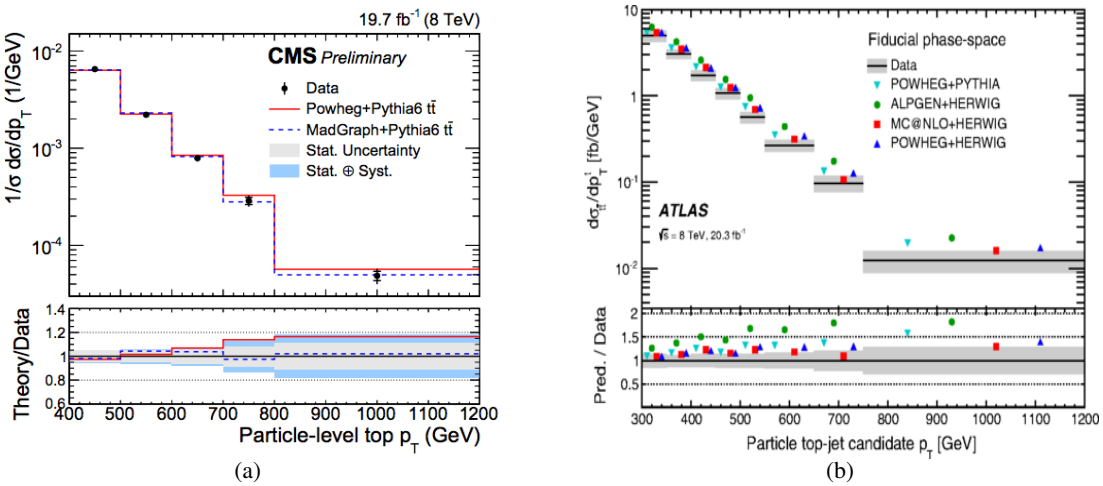

(a) (b)

Figure 5: $t\bar{t}$ production cross section as a function of the hadronic top quark p_T in the boosted regime from CMS (a) [13] and ATLAS (b) [16].

3. Differential $t\bar{t}$ production cross section

The CMS collaboration has already published the measurements of the $t\bar{t}$ differential cross section at 13 TeV with the 2015 data set (integrated luminosity of 2.3 fb^{-1}) [15]. The analysis is performed in the lepton-plus-jets decay channel selecting events with exactly one high energy lepton, at least four high transverse momentum jets, and at least one b-tagged jet.

Similar measurements are performed by the ATLAS collaboration at 8 TeV [16]. The event selection and and analysis strategy is similar for the two cases, allowing for independent but comparable results in the kinematic region where the top quarks have very high transverse momentum (boosted region). This boosted region should be treated separately due to its peculiar kinematic topology and gives information on the most interesting and less known part of the $t\bar{t}$ spectrum. It is also a useful probe for the gluon PDFs at high momentum.

The results from the two analyses are compatible in all the kinematic dependencies and in both the resolved and boosted regime as shown in Figure 5. Both analyses see an overestimation in the MC predictions, especially at high energies. A better agreement is found when using the new NNLO QCD predictions.

4. $t\bar{t}$ charge asymmetry

In proton-proton collisions at the LHC, the larger average momentum fraction of the valence quarks leads to an excess of top quarks produced in the forward and backward directions, while the antitop quarks are produced more centrally. The asymmetry observable is defined as

$$A_C = \frac{N(\Delta|y| > 0) - N(\Delta|y| < 0)}{N(\Delta|y| > 0) + N(\Delta|y| < 0)} \tag{4.1}$$

where $\Delta|y| = |y_t| - |y_{\bar{t}}|$ and y denotes the rapidity of the top and anti-top quarks. The measurement of this observable is not precise enough to establish the existence of the SM charge asymmetry yet but its high sensitivity to new physics makes this analysis very interesting.

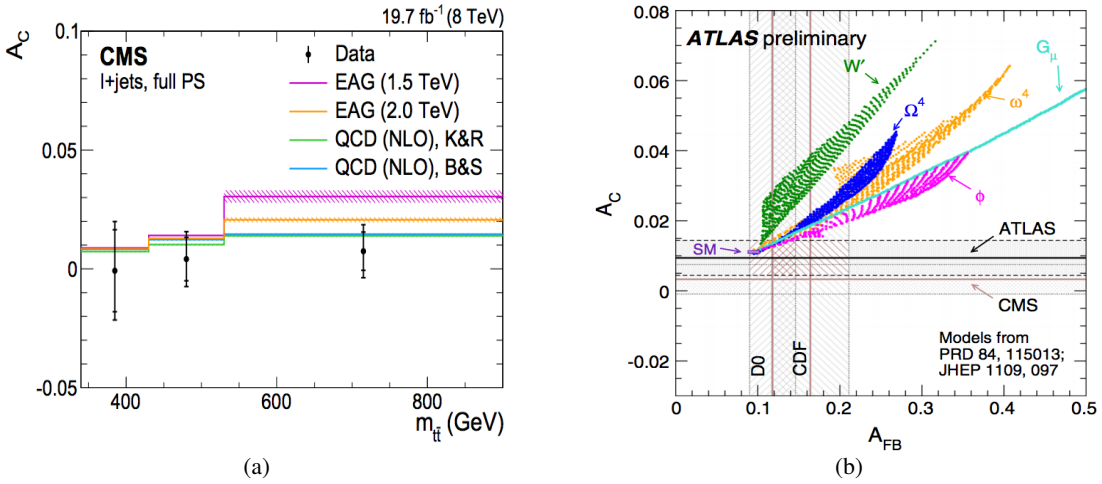

(a) (b)

Figure 6: (a) Distribution of the asymmetry observable A_C as a function of the $t\bar{t}$ mass [19] and (b) observed charged asymmetry compared with SM and BSM predictions [17].

Both the ATLAS [17][18] and CMS [19] collaborations have published results based on the data collected at a centre-of-mass energy of 8 TeV. The analyses are performed in the lepton-plus-jets channel and in both the resolved and boosted kinematic regime. The results are presented both at parton level and in a particle fiducial phase space defined with a selection as close as possible to the reconstruction one.

No deviations within two standard deviations from the Standard Model predictions are observed. These measurements, especially the boosted one, provide a constraint on extensions of the SM (Figure 6(b)).

5. Top quark polarization

The latest and more precise measurements of the polarization of the top quark and of the spin correlation of the $t\bar{t}$ system are performed in the di-lepton channel by both the ATLAS [20] and CMS [21][22] collaborations at $\sqrt{s} = 8$ TeV. Using the top quark polarization it is possible to estimate on the W_{tb} coupling element [23][24].

The polarization is evaluated from the angular distributions of the two leptons selected as coming from the top decay, both inclusively and differentially, with respect to different kinematic variables. Different observables are used to obtain unambiguous results. The principal ones are the angle θ_l* between the lepton and its parent top quark and the ϕ angle between the two leptons. These are evaluated in the top rest frame and in the laboratory frame respectively.

The measured top quark polarization and the spin correlation observables are compared to theoretical predictions in order to search for hypothetical top quark anomalous couplings (Figures 7). No evidence of new physics is observed allowing to place more stringent constrains upon Beyond SM theories. The limit fixed on the W_{tb} coupling element is also in agreement with the Standard Model prediction.

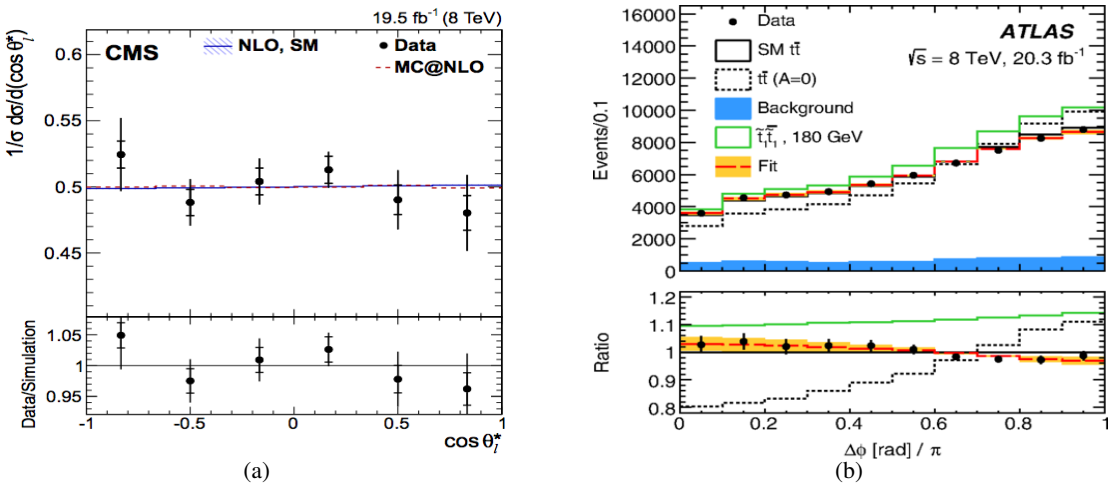

Figure 7: Distributions of the top polarization angles $cos(\theta*)$ (a) [24] and ϕ_l (b) [23].

6. Single top quarks

Top quarks can be singly produced in proton-proton collisions via charged-current electroweak interactions. Three mechanisms contribute to single-top-quark production in the standard model, referred to as the t, s and W-associated, or tW, channels. In proton-proton collisions at the Large Hadron Collider the t channel mode is by far the most abundant of the three. The study of single-top-quark production provides a unique possibility to investigate many aspects of top-quark physics that cannot be easily probed in $t\bar{t}$ production: one can investigate the tWb vertex structure looking for anomalous couplings [25] and flavour-changing neutral current (FCNC) contributions [26] in the production. Moreover, the cross-sections of all three channels are directly related to the modulus squared of the Cabibbo-Kobayashi-Maskawa matrix element V_{tb}.

A summary of single-top-quark cross-section measurements is found in fig 8(a), while $|V_{tb}|$ measurements are shown in Fig. 8(b). No deviation from the Standard Model prediction is observed.

6.1 t channel

Single-top-quark production in the t channel yields the highest cross section amongst the three production modes. First measurements of t channel cross section at 13 TeV were performed by ATLAS [27] and CMS [28], already reaching a systematics dominated regime. For both experiments, a selection is applied with two or three jets, one or two of which passing a b-tagging requirement. The main background processes are top pair production, W bosons associated to jets, and QCD multijet production. Multivariate discriminants, shown in Fig. 9(a), 9(b) for ATLAS and CMS respectively, are used to discriminate the t channel signal from the aforementioned processes.

The measured cross sections at 13 TeV result 229 ± 48 pb (ATLAS) and 228 ± 33 pb (CMS).

6.2 tW associated production

Top quarks singly produced in association with W bosons allow for a complementary route for new physics searches in the single-top-quark sector. This process was observed for the first time in

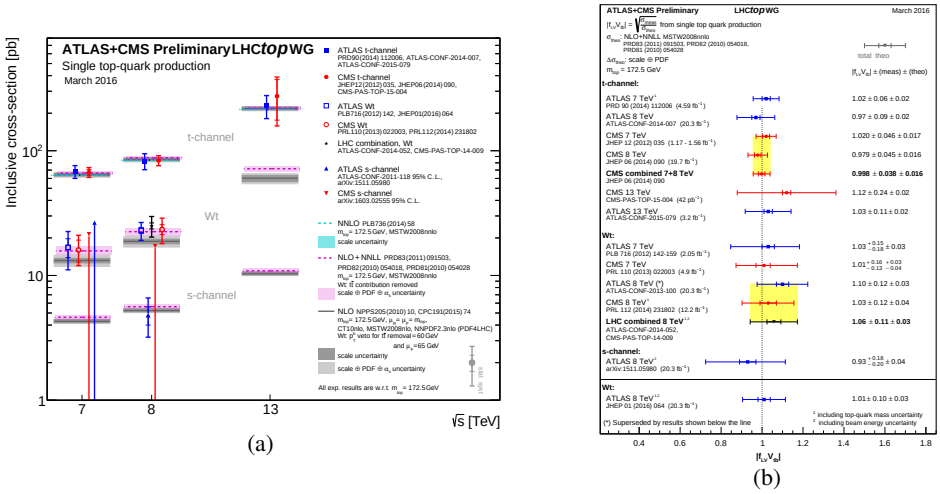

(a) (b)

Figure 8: Single-top-quark production cross-section measurements at LHC as a function of the centre-of-mass energy(a) and measurements of $|V_{tb}|$from inclusive single-top-quark cross section(b) [36].

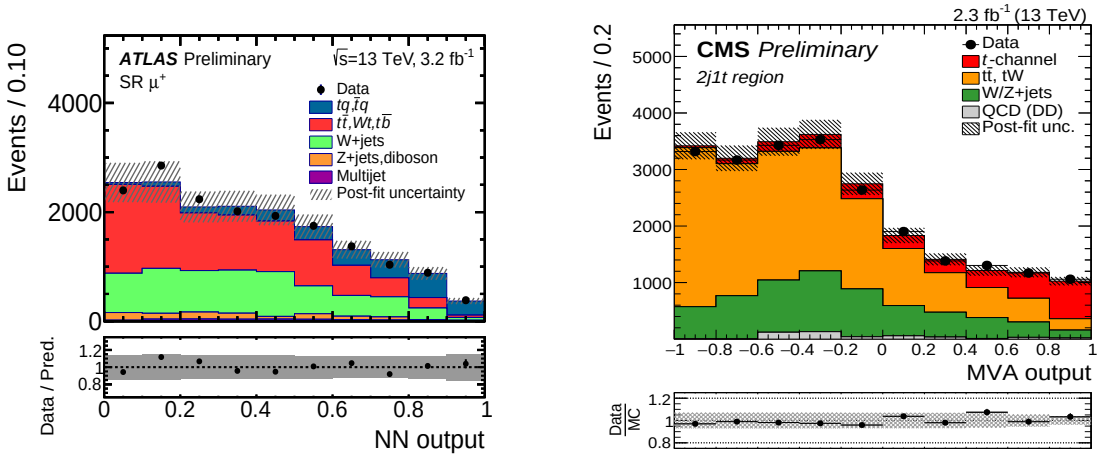

(a) (b)

Figure 9: Discriminating observable used for t channel single-top-quark production cross section extraction for ATLAS(a), the output discriminator of a boosted decision tree Method(a) [27], and for CMS, the output discriminator of a neural network(b) [28], at 13 TeV.

2014 by CMS [29], and subsequently by ATLAS [30]. A selection with 2 leptons, either electrons or muons, is performed to define a signal enriched region and a fit to a respective multivariate discriminants, displayed in Fig. 10, is performed for both analsyses.

The measured cross sections at 8 TeV are 23.0 $\pm$ 3.6 (ATLAS) and 23.4$\pm$ 5.4 (CMS).

6.3 *s* channel

The most rare of the three production modes for single-top is the *s* channel. Both ATLAS [31] and CMS [32] have performed searches for this channel at LHC in Run-I, looking for events with 1 lepton and 2 jets stemming from b hadronisation in the final state. The ATLAS measurement resulted in the first evidence for the process at LHC, with an observed(expected) significance of

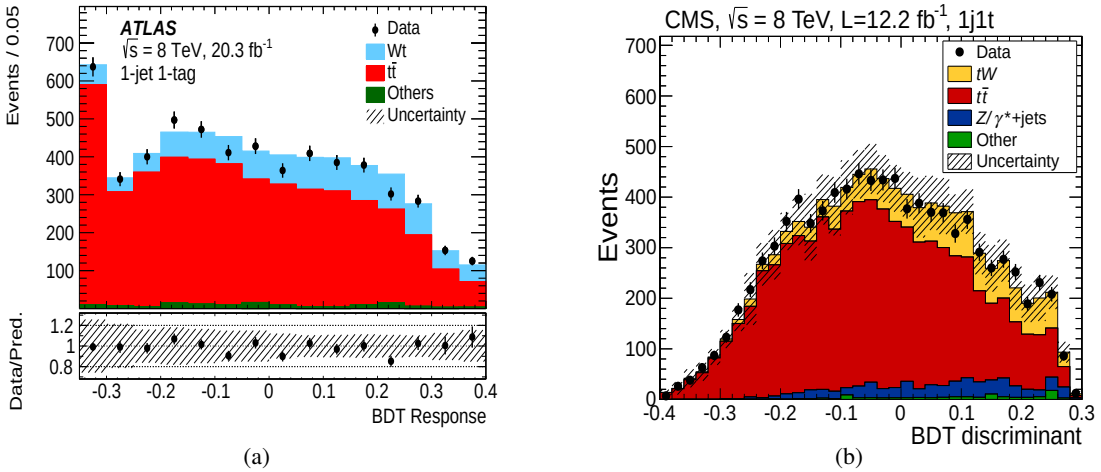

(a) (b)

Figure 10: Discriminating observable used for W-associated single-top-quark production cross section extraction for CMS(a) [29] and ATLAS(b) [30] at 8 TeV). In both cases it is the output discriminator of a boosted decision tree.

3.2(3.9) standard deviations. The discriminating variables used for signal extraction in the two analyses, a matrix element discriminant for ATLAS, and a multivariate discriminant for CMS, are shown in Fig. 11(a) and 11(b) respectively.

The measured cross sections at 8 and 7 TeV are:

$$\sigma^{8\mathrm{TeV}}_{s-\mathrm{channel}} = 4.8 \pm 0.8(\mathrm{stat})^{+1.6}_{-1.3}(\mathrm{syst})\mathrm{pb}, (\mathrm{ATLAS})$$
$$\sigma^{8\mathrm{TeV}}_{s-\mathrm{channel}} = 13.4 \pm 7.3(stat+syst)\mathrm{pb}, (\mathrm{CMS})$$
$$\sigma^{7\mathrm{TeV}}_{s-\mathrm{channel}} = 7.1 \pm 8.1(stat+syst)\mathrm{pb}, (\mathrm{CMS})$$

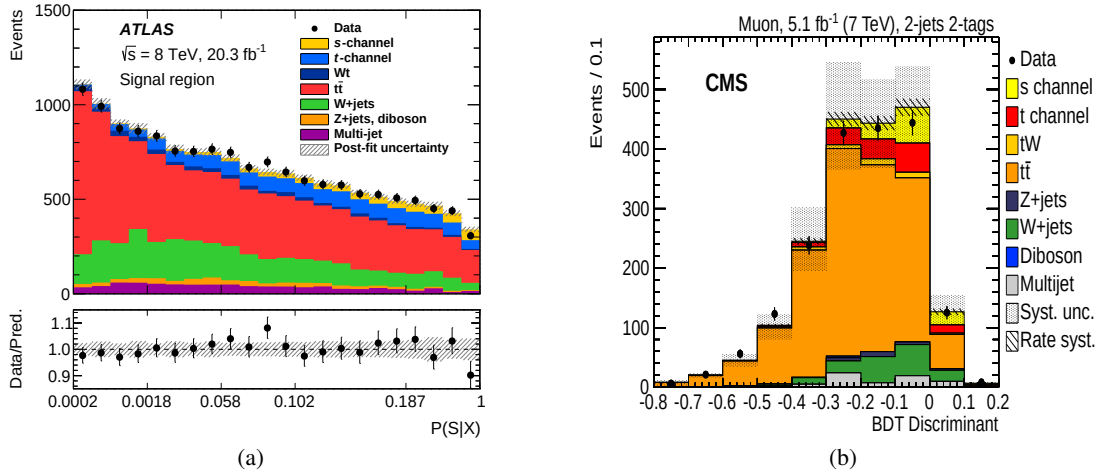

(a) (b)

Figure 11: Discriminating observable used for *s* channel single-top-quark production cross section extraction for ATLAS at 8 TeV, a Matrix Element Method output discriminator (a) [31], and CMS at 7 TeV, a boosted decision tree output discriminator (b) [32].

7. Top quark mass measurements

Precise measurements of the top quark mass are of crucial importance as it constitutes one of the fundamental Standard Model parameters. Since top quark decays via weak interaction, it is possible to have access to its decay products in order to define observables sensitive to the top quark mass, making it possible to determine it at the percent level. Measurements from LHC Run-I are leading in terms of precision, as they can profit from the detector calibrations obtained over the course of the years.

The most precise single measurements from ATLAS[33] and CMS[34] are based on 8 TeV data, and extract simultaneously the top quark mass together with the jet energy scale from $t\bar{t}$. The most precise CMS measurement[34] exploits the semi-leptonic decay channel, requiring one lepton and at least four jets, hadronically decaying top quark from three jets. A kinematic fit is performed to each jet permutation forming the hadronically decaying top quark. The goodness of fit probability for all possible permutations is used to construct an event-by-event likelihood and to measure the top quark mass. The most precise ATLAS[33] measurement exploits the dileptonic decay channel, requiring two leptons and two b-jets. retaining the permutation with the lowest invariant mass possible of the two lepton-b-jet pair. The resulting measured top quark mass is for the two cases:

$$m_{top} = 172.99 \pm 0.41(\text{stat}) \pm 0.74(\text{syst})\text{GeV}, (\text{ATLAS})$$
$$m_{top} = 172.35 \pm 0.16(\text{stat}+\text{jsf}) \pm 0.48(\text{syst})\text{GeV}, (\text{CMS}).$$

The variables used in the mass extraction for the two cases are shown in Fig. 12(a), 12(b), respectively for ATLAS and CMS.

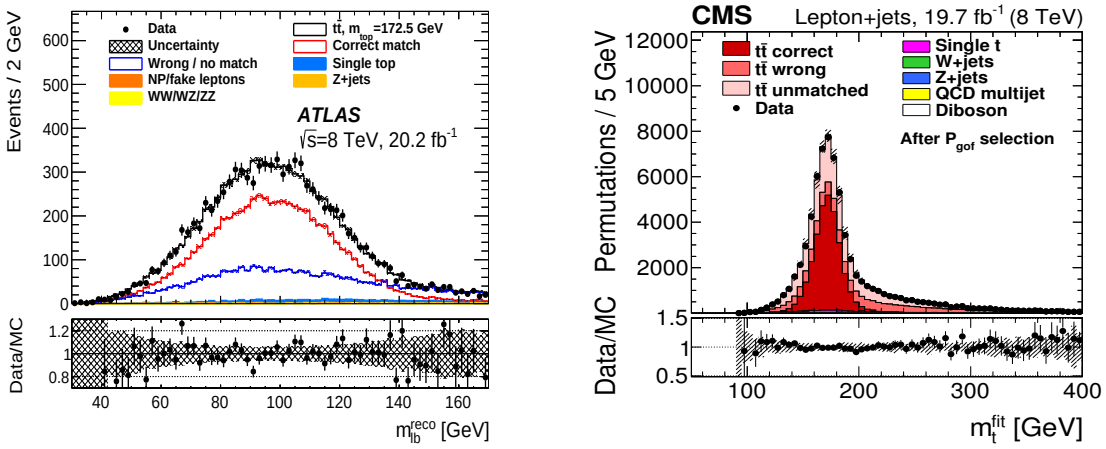

(a) (b)

Figure 12: Mass of the lepton-b-jet pair from ATLAS [33], mass of the three jets from the best permutation from CMS [34].

The main systematic uncertainty sources for the above methods come from the b hadronisation model and the color reconnection model. Several top quark mass measurements are performed by the different experiments with different techniques. While they lead to an overall lower precsion

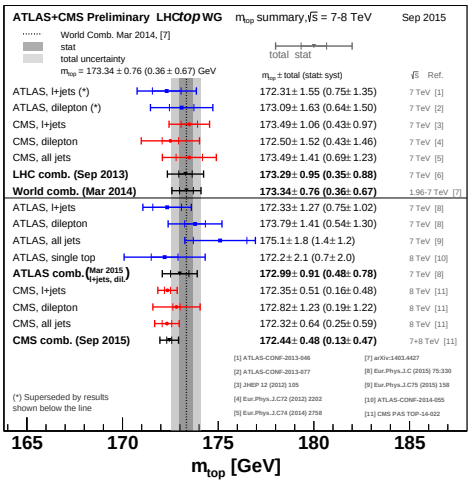

(a)

Figure 13: Overview of the most precise single measurements of the top quark mass and top quark mass combinations [36].

for the single-measurement with respect to the two above mentioned, they allow to gain precision in a combination.

The ultimate goal is to combine all measurements across different experiments to achieve the best possible precision. A world-wide combination is performed within the LHCTopWG [35]. An overview of the LHC measurements is shown in Fig. 13.

References

[1] M. Czakon, P. Fiedler and A. Mitov, Phys. Rev. Lett. **110**, 252004 (2013) doi:10.1103/PhysRevLett.110.252004 [arXiv:1303.6254 [hep-ph]].

[2] G. Aad *et al.* [ATLAS Collaboration], JINST, 3 (2008) S08003

[3] V. Khachatryan *et al.* [CMS Collaboration], JINST, 3 (2008) S08004

[4] R. Aaij *et al.*, [LHCb Collaboration], JINST, 3 (2008) S08005

[5] G. Aad *et al.* [ATLAS Collaboration], Eur. Phys. J. C **74**, no. 10, 3109 (2014) doi:10.1140/epjc/s10052-014-3109-7 [arXiv:1406.5375 [hep-ex]].

[6] M. Aaboud *et al.* [ATLAS Collaboration], Phys. Lett. B **761** (2016) 136, doi:10.1016/j.physletb.2016.08.019.

[7] ATLAS collaboration [ATLAS Collaboration], ATLAS-CONF-2015-049.

[8] V. Khachatryan *et al.* [CMS Collaboration], [arXiv:1603.02303 [hep-ex]].

[9] V. Khachatryan *et al.* [CMS Collaboration], CMS-PAS-TOP-16-005.

[10] R. Aaij *et al.* [LHCb Collaboration], Phys. Rev. Lett. **115**, no. 11, 112001 (2015) doi:10.1103/PhysRevLett.115.112001 [arXiv:1506.00903 [hep-ex]].

[11] R. Aaij *et al.* [LHCb Collaboration], JINST **10**, no. 06, P06013 (2015) doi:10.1088/1748-0221/10/06/P06013 [arXiv:1504.07670 [hep-ex]].

[12] The ATLAS collaboration, ATLAS-CONF-2015-065.

[13] V. Khachatryan *et al.* [CMS Collaboration], CMS-PAS-TOP-16-008.

[14] V. Khachatryan *et al.* [CMS Collaboration], CMS-PAS-TOP-16-011.

[15] V. Khachatryan *et al.* [CMS Collaboration], CMS-PAS-TOP-14-012.

[16] G. Aad *et al.* [ATLAS Collaboration], Phys. Rev. D **93** (2016) no.3, 032009 doi:10.1103/PhysRevD.93.032009 [arXiv:1510.03818 [hep-ex]].

[17] G. Aad *et al.* [ATLAS Collaboration], Eur. Phys. J. C **76** (2016) no.2, 87 doi:10.1140/epjc/s10052-016-3910-6 [arXiv:1509.02358 [hep-ex]].

[18] G. Aad *et al.* [ATLAS Collaboration], Phys. Lett. B **756** (2016) 52 doi:10.1016/j.physletb.2016.02.055 [arXiv:1512.06092 [hep-ex]].

[19] V. Khachatryan *et al.* [CMS Collaboration], Phys. Lett. B **757** (2016) 154 doi:10.1016/j.physletb.2016.03.060 [arXiv:1507.03119 [hep-ex]].

[20] G. Aad *et al.* [ATLAS Collaboration], Phys. Rev. Lett. **114** (2015) no.14, 142001 doi:10.1103/PhysRevLett.114.142001 [arXiv:1412.4742 [hep-ex]].

[21] V. Khachatryan *et al.* [CMS Collaboration], Phys. Rev. D **93** (2016) no.5, 052007 doi:10.1103/PhysRevD.93.052007 [arXiv:1601.01107 [hep-ex]].

[22] V. Khachatryan *et al.* [CMS Collaboration], JHEP **1604**, 073 (2016) doi:10.1007/JHEP04(2016)073 [arXiv:1511.02138 [hep-ex]].

[23] [ATLAS Collaboration], ATLAS-CONF-2013-032.

[24] V. Khachatryan *et al.* [CMS Collaboration], CMS-PAS-TOP-16-001.

[25] Single top quark production at LHC with anomalous Wtb couplings, Aguilar-Saavedra, J.,Nucl. Phys. B 804 (2008) 160-192

[26] Search for anomalous top quark production at the early LHC, Gao, J. et al., Phys. Rev. Lett. 107 (2011) 092002.

[27] [ATLAS Collaboration], ATLAS-CONF-2015-079.

[28] V. Khachatryan *et al.* [CMS Collaboration], CMS-PAS-TOP-16-003.

[29] V. Khachatryan *et al.* [CMS Collaboration], PRL 112,231802.

[30] G. Aad *et al.* [ATLAS Collaboration], JHEP01(2016)064.

[31] G. Aad *et al.* [ATLAS Collaboration], Phys.Lett.B(2016)228-246.

[32] V. Khachatryan *et al.* [CMS Collaboration], arXiv:1603.02555.

[33] G. Aad *et al.* [ATLAS Collaboration], arXiv:1606.02179.

[34] V. Khachatryan *et al.* [CMS Collaboration], arXiv:1509.04044.

[35] The ATLAS, CMS, CDF, and D0 Collaborations, arXiv:1403.4427.

[36] The LHC Top Working group, LHCTopWG summary plots, https://twiki.cern.ch/twiki/bin/view/LHCPhysics/LHCTopWG